Estuarine, Coastal and Shelf Science (1988) **26**, 285–308

The Deepwater Exchange Cycle in Indian Arm, British Columbia

Brad de Young[a] **and Stephen Pond**

Department of Oceanography, University of British Columbia, Vancouver, British Columbia, V6T 1W5, Canada

Received 15 September 1986 and in revised form September 1987

Keywords: fjords; estuarine circulation; diffusion; mixing; hydraulic models; British Columbia Coast

A silled fjord on the British Columbia coast, Indian Arm, was used to study the exchange processes controlling deepwater exchange in fjords. Bottom-water renewal took place during the winter of 1984/85. Hydraulic control of the exchange is exerted over the long sill which restricts access to the fjord. The maximum density at the sill occurs during neap tides. No distinct peaks in the velocity at the sill are observed during periods of inflow. Reduced vertical mixing over the long sill during periods of neap tides sets the timing of the bottom water exchange. During each inflow over the 1984/85 winter about 20% of the water in the fjord was replaced. These exchanges occurred over periods of 5–10 days. Between the exchange years, diffusion of the water in the basin is important in conditioning the water for the next exchange event. The vertical diffusion coefficient (K_v) was determined from an analysis of the salinity data and was found to be related to the buoyancy frequency N by the relationship, $K_v \propto N^{-1.6}$.

Introduction

Captain George Vancouver, after a night anchored in Port Moody, passed the narrows of Indian Arm in 1792 and concluded that it did not provide a navigable route to Europe because of its weak tidal flow. Partly because of its proximity to Vancouver, Indian Arm has been much studied. The irregular deepwater exchange cycle and the near anoxic bottom water have provided the main interest. Deepwater renewal in fjords has been discussed extensively in two recent reviews: Gade and Edwards (1980) focus on deepwater exchange and its effects upon the circulation and, in a more general review of fjord oceanography, Farmer and Freeland (1983) also discuss renewal.

A fairly complete ' classical ' description of Indian Arm, based primarily upon bottle-cast data, was presented by Gilmartin (1962). Davidson (1979) provided observations of an exchange event over the 1974/75 winter. Burling (1982) reviewed the earlier work and placed the studies within the context of other work on deepwater renewal in fjords. Dunbar (1985) developed a tidal numerical model of the fjord. A discussion of the internal

[a]Present address: Department of Fisheries and Oceans, Bedford Institute of Oceanography, P.O. Box 1006, Dartmouth, Nova Scotia, B2Y 4A2, Canada.

0272–7714/88/030285+24 $03.00/0

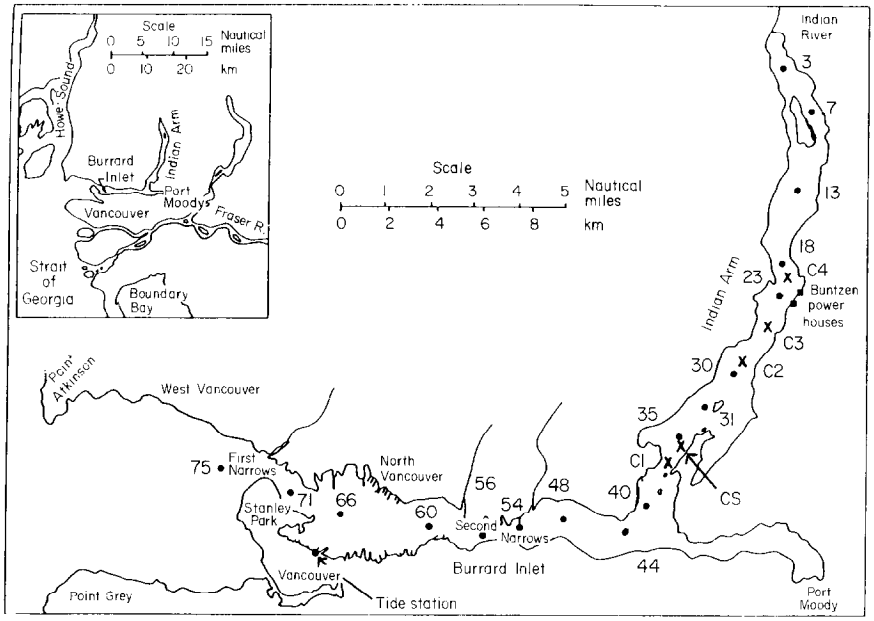

Figure 1. Map of Burrard Inlet and Indian Arm showing the station locations. (●) CTD stations; (×) current-meter stations.

tide (de Young & Pond, 1987) serves as a complement to this paper. New, more detailed data on the exchange are presented here. Using these data, a better understanding is developed of the dynamics of the exchange process in Indian Arm.

The position and bottom topography of Indian Arm are shown in Figures 1 and 2; it is a long, narrow fjord with a deep basin separated from the Strait of Georgia by a series of sills in Burrard Inlet. Three sills can be identified in Figure 2 although, because Burrard Inlet is so shallow, almost all of it can be considered a sill of Indian Arm. CTD data were collected monthly for the 1983/84 and 1984/85 winters (de Young, 1986). Cyclesonde profiling current meter CTD systems (van Leer *et al.*, 1974) were used at the two stations C1 and C3 for the winters of 1982–1985. Only data from the 1984/85 winter, when deepwater exchanged occurred, will be presented here. All the current meters were calibrated for temperature and salinity before and after each field season. The CTD data were collected using a Guildline Model 8705 digital probe. Regular calibration checks indicate the error limits for the CTD data to be: $T \pm 0{\cdot}01$ °C, $S \pm 0{\cdot}01$, and $\sigma_t \pm 0{\cdot}01$. Unless stated otherwise, density is given as σ_t.

Density structure and diffusion

The basic features of Indian Arm, first described in detail by Gilmartin (1962), are illustrated in the contour plot of temperature, density (σ_t) and salinity presented in Figure 2. There is a thin surface layer 1–3 m thick which overlies a strong halocline between 3 and 5 m. Below this layer the salinity gradually increases towards the bottom, where the stratification is weak. The dynamical effects of the surface layer are weak. Dunbar (1985) was able to create an effective tidal numerical model of the system using a vertical grid

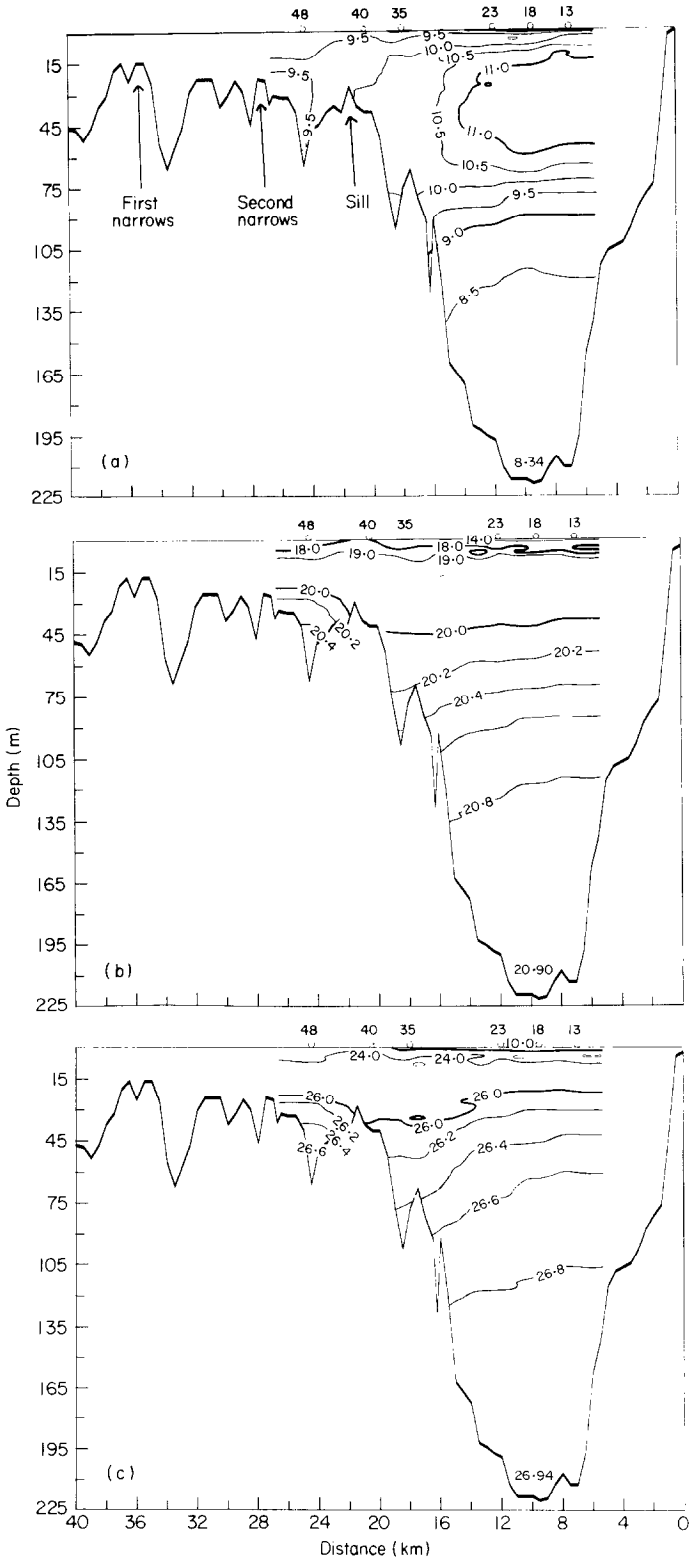

Figure 2. Contours of (a) temperature in °C, (b) σ_t and (c) salinity along Indian Arm on 7 November 1984. The station numbers where the data were collected (see Figure 1) are indicated at the top of the plots.

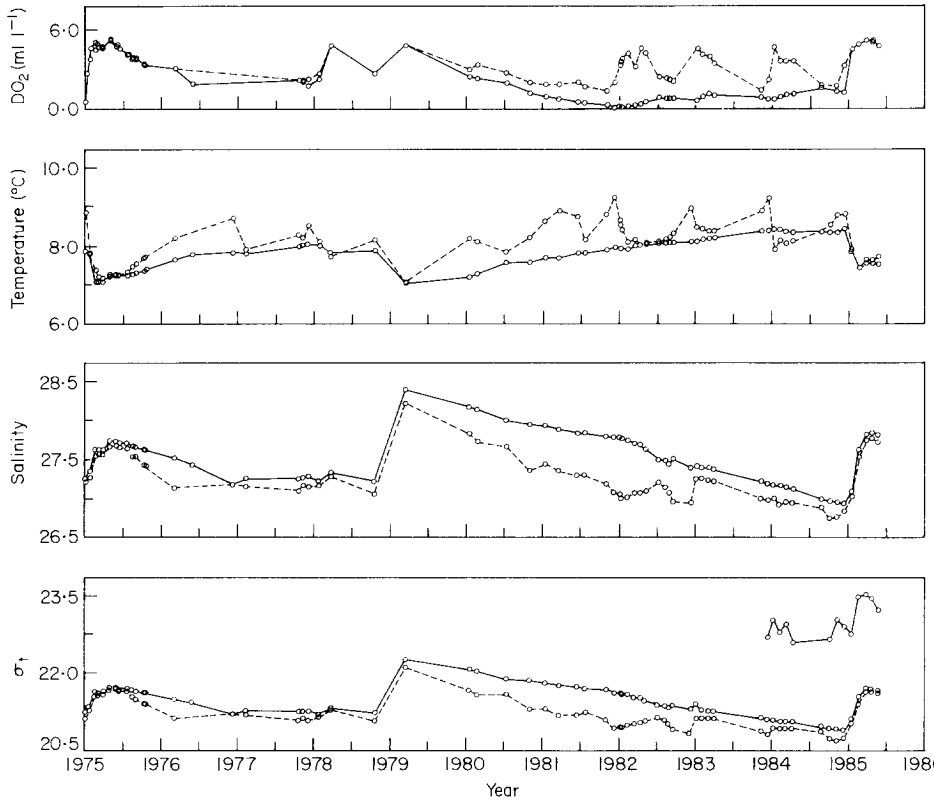

Figure 3. Time series of dissolved oxygen concentration DO_2, temperature, salinity and σ_t at station 23 in Indian Arm. (———) Data at 200 m; (- - -) data at 100 m. The extra density data at the end (1984–1985) are from 40 m depth at station 75 outside First Narrows.

spacing of 10 m. From Knudsen's relations the estuarine flow velocity at the sill is about 2 cm^{-1}, which is insignificant compared to the tidal velocity of 50 cm^{-1}.

The surface layer is thin because of the small freshwater input. The total annual freshwater flow averages 42 $m^3 s^{-1}$; 23 $m^3 s^{-1}$ comes from the Buntzen power plants which are situated 12 km from the head of the inlet. The majority of the remainder (12 $m^3 s^{-1}$) comes from the Indian River (Figure 1). In a comparison with other British Columbia fjords, Pickard (1961) classified Indian Arm as a low runoff inlet.

The deepwater conditions in the fjord are determined by quasi-periodic intrusions of water from outside the inlet. Figure 2 shows that the properties of water reaching the Indian Arm sill are strongly influenced by the passage of water through Burrard Inlet. The two sills in Burrard Inlet, at First and Second Narrows may hydraulically control the flow of water through Burrard Inlet. In Burrard Inlet then, there are two important effects: vertical mixing of the inflowing water and hydraulic control of the exchange.

The water properties at two depths in the basin of Indian Arm, from 1975–1986, are shown in Figure 3. Four renewal events took place during the 11-year period: 1974/75, 1977/78, 1978/79 and 1984/85. Usually the bottom water renewals are indicated by an increase in the water density at 200 m. During the 1977/78 exchange only a small increase in the density of the bottom water was observed, however, a large increase in the dissolved

oxygen concentration occurred. An increase in the oxygen concentration of the bottom water, which decreases between exchange periods, is associated with each exchange event.

The saw-toothed shape of the time series in Figure 3 is common to many fjords (Pickard, 1975). Following an exchange event, the water properties show a steady decrease (or increase, depending on the sign of the vertical gradient) until the next exchange. The variations are more irregular at 100 m than at 200 m because of the more frequent mid-depth exchanges of water. Advection of new water disrupts the diffusion process. The diffusion at 200 m is such that the salinity changes at an approximately fixed rate.

Diffusion in seawater is complex because (a) both temperature and salt diffuse and (b) the energy for diffusion comes from turbulence. The first aspect leads to complexity because density is a function of the diffusion of two properties which differ in their rates of diffusion. All diffusion must ultimately take place at the molecular level but the overall rate may be controlled by turbulence which means that the observed rate of diffusion is larger than the molecular rates of diffusion. The diffusion equation is

$$\frac{\mathrm{D}S}{\mathrm{D}t} = \frac{\partial}{\partial x}\left(K_h \frac{\partial S}{\partial x}\right) + \frac{\partial}{\partial y}\left(K_h \frac{\partial S}{\partial y}\right) + \frac{\partial}{\partial z}\left(K_v \frac{\partial S}{\partial z}\right), \tag{1}$$

where S is the salinity, K_h is the coefficient of horizontal diffusivity and K_v is the coefficient of vertical diffusivity. It is assumed that the process controlling horizontal diffusion is different from that driving the vertical diffusion. In a fjord, which is relatively homogeneous in the horizontal, it is assumed that the first two terms on the right side can be neglected. The assumption that $\partial S/\partial y$ (where y is across the channel) is zero is probably quite good. The assumption that $\partial S/\partial x$ is zero, is probably not as good because there is a long channel gradient, the result of freshwater inflow although in the deeper water this gradient is also small. It is also assumed that there are periods when there is negligible advective contribution to diffusion, so the total derivative on the left side of equation (1) becomes a partial derivative.

It has often been assumed that K_v is a constant independent of depth, however, recent work suggests that K_v is not a constant but is a function of the stratification (Osborn, 1980; Gargett, 1984). Gargett and Holloway (1984) suggest that all systems in which the energy source is turbulence from internal waves should exhibit an inverse linear relationship between K_v and N. They review observations of the rate of kinetic energy dissipation and find that it tends to vary systematically with the buoyancy frequency N. At steady state, they equate the dissipation rate to the sum of the mechanical production of energy and the energy which does work against buoyancy. From the definitions of R_f and K_v

$$K_v = \frac{R_f}{1 - R_f} \varepsilon N^{-2}, \tag{2}$$

where R_f is the flux Richardson number and ε is the kinematic energy dissipation. The flux Richardson number is defined as the ratio of the energy flux working against buoyancy over the total mechanical production of energy. Following an analysis of the steady-state energy equation, Gargett and Holloway (1984) show that the dissipation is

$$\varepsilon = \varepsilon_0 N^{-p}, \tag{3}$$

where $p = 1$ if all of the waves are of a single frequency and $p = 1{\cdot}5$ if the waves exhibit the broad-band oceanic spectrum (Munk, 1981). The parameter ε_0 is a site-specific constant which depends on the energy level of the local internal wave field. If the flux Richardson number is constant, then equation (2) becomes

$$K_v = a_0 N^{-2+p} = a_0 N^{-q} \tag{4}$$

where $0{\cdot}5 < q < 1{\cdot}0$. In equation (4), a_0 is a site-specific constant, related to ε_0 by R_f, which is also dependent on the energy in the local internal wave field.

In Indian Arm, an investigation of diffusion is important for several reasons. First, diffusion is important in the exchange process in that it serves to condition the water between exchanges, reducing the density of the bottom water by the diffusion of salt. Second, diffusion is an important measure of the level of turbulence in the system. It is also an important sink of the internal wave energy which is generated at the sill (Stigebrandt, 1976, 1980). An improved understanding of diffusion in fjords is also necessary for the development of numerical models of fjord circulation (Dunbar, 1985).

The coefficient of diffusion is determined by solving equation (1), with the horizontal terms dropped, using measurements of the salinity or temperature in the fjord. This technique is referred to as the budget method. It assumes that there are no sources or sinks. Temperature does not fulfill this condition as well as salinity, because heating and cooling occur near the surface, and, therefore, the results for temperature may not be as good. Equation (1) is solved by integrating from the bottom at $z = 0$ to some height h:

$$K_v(h) = \frac{\dfrac{\partial}{\partial t}\displaystyle\int_0^h A(z)\, S \mathrm{d}z}{\dfrac{\partial S}{\partial z} A(h)} . \tag{5}$$

The area of the inlet $A(z)$ at each level must be included to account for the changing volume of water with depth. It is necessary to ensure that during the period of integration there is no advection of salt into Indian Arm. The cyclesonde data show when there is no exchange in the fjord. The CTD data were averaged over 10-m intervals. The 10 m depth range is large enough to remove the internal waves, but still small enough to allow reasonable vertical resolution.

The period chosen for the diffusion analysis in Indian Arm was January–March 1983, when there was minimal exchange. Results from the analysis are presented in Figure 4(a) for both the temperature and the salinity. The generally small temperature gradient may be the cause of the noisier plot for temperature. The least-squares fit for the salinity data gives a slope

$$K_v \propto N^{-1{\cdot}6}. \tag{6}$$

The slope for temperature is $-1{\cdot}2$. The least-squares fit presented is the average of K_v versus N^2 and N^2 versus K_v. Such an average gives equal weighting to the errors in each variable fitted. For comparison, a solid line of slope $K_v \propto N^{-1}$ is drawn at the bottom of the plot. The data from the shallower depths, where N is larger, appear to have a slope closer to -1 than does the entire set of points.

Data from Saanich Inlet on Vancouver Island were also analysed using this same technique. Although no current-meter data are available to determine the exchange conditions, the anoxic water at the bottom of the inlet does provide a good test of exchange (Anderson & Devol, 1973). Results of the analysis for November–December 1984 are

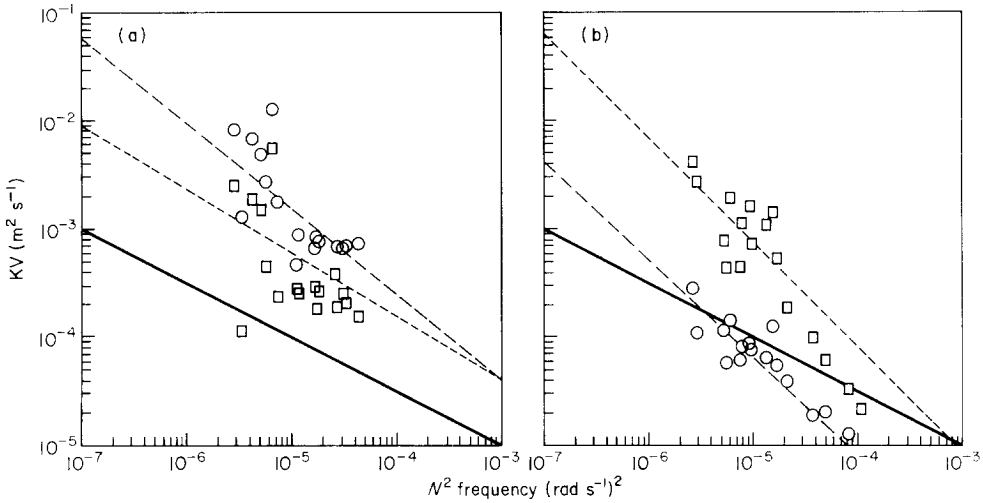

Figure 4. K_v versus N^2 in (a) Indian Arm (5 January–29 March 1983) and (b) Saanich Inlet (8 November–13 December 1984). The depth range for both plots is 100–185 m. ○, Salinity; □, temperature. The long-dashed (salinity) and short-dashed (temperature) lines are least-squares fits. The solid line shows a $K_v \propto N^{-1}$.

presented in Figure 4(b). The slope for the Saanich Inlet analysis is −1·8 for salinity and −1·9 for temperature. The larger range of N^2 makes the fitted line more robust.

The results in Indian Arm provide some support for the suggested relationship between K_v and N of Gargett and Holloway (1984) and Gargett (1984). According to their work, a slope of −1 indicates that the diffusion is primarily driven by internal-wave dissipation and that the internal waves are primarily of one frequency. The slope in Indian Arm is, however, steeper than −1 over the whole range of N and the slope in Saanich Inlet is clearly much steeper than −1, indeed it is almost −2. There is other observational evidence for a slope steeper than −1. Gade and Edwards (1980), for instance, found a mean slope of −1·6 in Oslofjord with large differences from basin to basin. Lewis and Perkin (1982) found a slope of −1·2 in a Greenland fjord. Their result suggests a different energy source for the mixing. If the energy source for the mixing is not internal-wave dissipation, then the suggested relationship between K_v and N may not hold. Wind mixing and vertical convection driven by winter cooling may be more important buoyancy sources in some fjords. In summary, the general prediction of Gargett and Holloway, suggesting a $K_v \propto N^{-q}$ relationship, is supported. The value of q in fjords appears to be greater than suggested by their theory.

The exchange cycle

Little change was observed in the basin water properties from October to November 1984. There was, however, an increase of 0·2 in the density at the bottom of station 48. By December 1984 (Figure 5), the density at this position just outside the Indian Arm sill increased further to 20·6, from 20·2 in October. During this period, there was a general decrease in the stratification below 10 m. The change in the deep water properties is most apparent in the temperature contour plot [Figure 5(a)]. The salinity plots have been

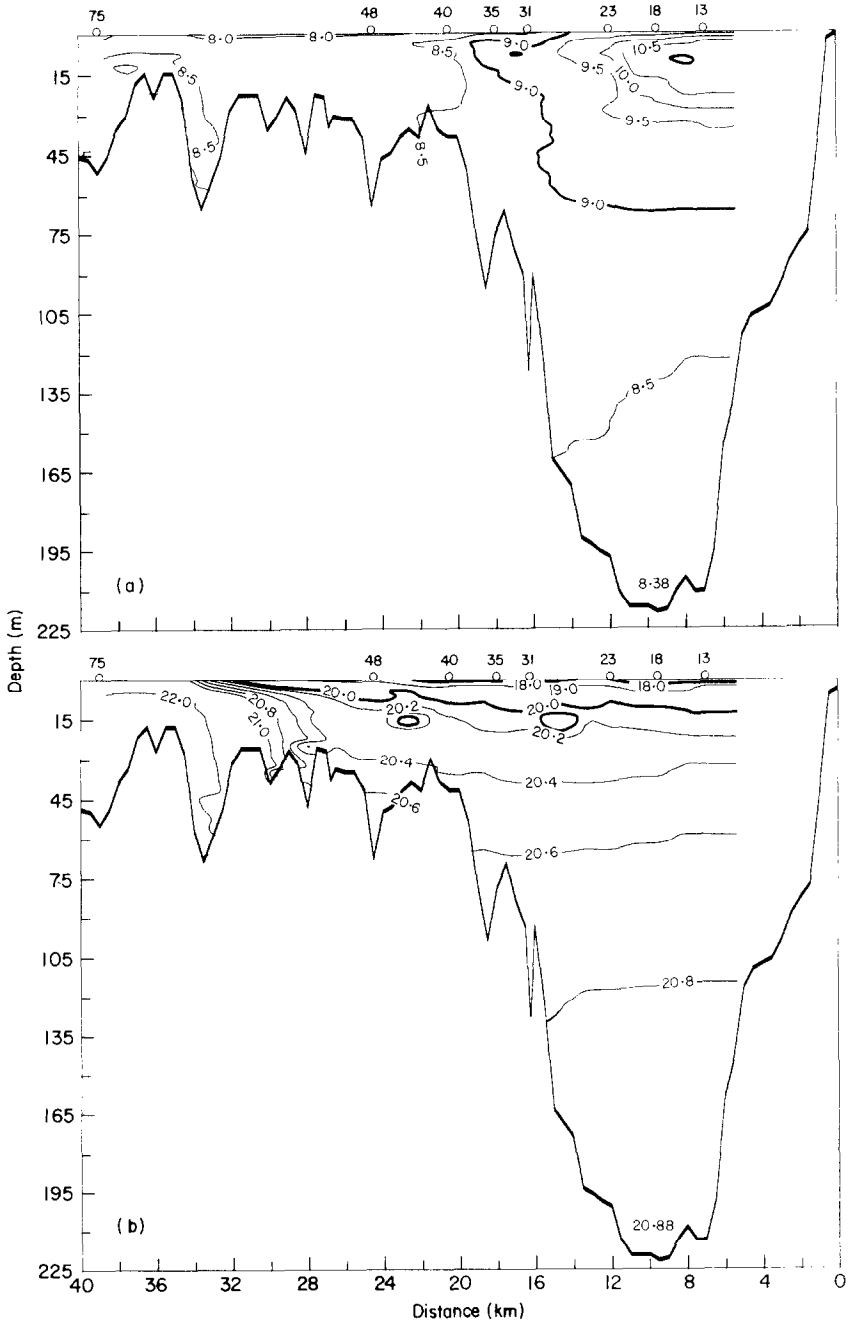

Figure 5. Temperature (a) and σ_t (b) along Indian Arm on 11 December 1984. The station numbers where the data were collected are indicated at the top of the plots.

dropped from further discussion because they provide no additional information to the density plots as the density of the water is controlled primarily by the salinity.

Figure 6 shows that from December to January the bottom water density had increased by 0·20. The bottom temperature had decreased by 0·57 °C. The density plot shows an

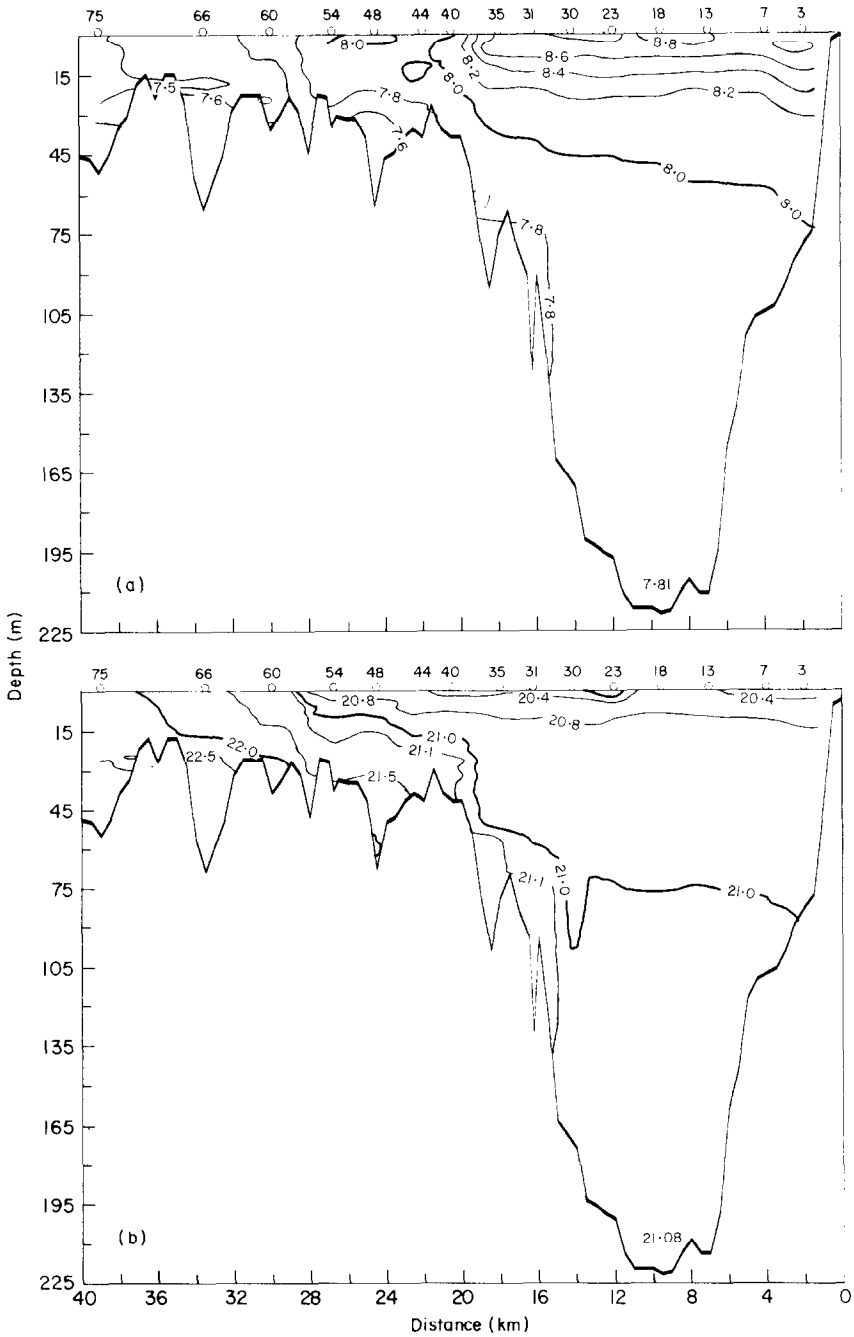

Figure 6. Temperature (a) and σ_t (b) along Indian Arm on 15 January 1985. The station numbers where the data were collected are indicated at the top of the plots.

unstable tongue of water extending over the sill into Indian Arm. For instance the 21·0 isopycnal at station 30 looks as if it were being drawn downward by the inflow and the density at the bottom of station 48 (greater than 21·5) was more than 0·4 higher than the density at the bottom of the basin. The exchange also weakens the stratification in the

basin. From the bottom to 15 m depth, the density difference before the exchange was 0·9. After the exchange the density difference was 0·28.

This bottom water flushing also influenced the dissolved oxygen concentration (DO_2) in the basin. Prior to the exchange the DO_2 above 50 m was greater than 3 ml l^{-1}; below 100 m it was less than 2 ml l^{-1}. The lowest oxygen concentration in December was about 1·0 ml l^{-1} near the bottom. Following the exchange, in January 1985, the DO_2 level at 15 m was less than 2 ml l^{-1}. Below this depth the concentration was greater than 4 ml l^{-1}. Low-oxygen water was displaced upwards by the inflow of oxygen-rich water.

The effects of further inflow can be seen in the February 1985 plots (see Figure 7). The density of the bottom water increased to 21·55. Water at the sill (21·7) was still more dense than that at the bottom of the fjord. The horizontal density gradient through Burrard Inlet was still strong with several subsurface fronts visible in Figure 7. These fronts indicate the importance of mixing and hydraulic effects through Burrard Inlet.

The vertical temperature gradient near the bottom which in February was positive (Figure 7) was negative by March. The density at the bottom of station 48 was somewhat less than that at the bottom of the fjord indicating no inflow at the time of the CTD survey. The strong horizontal gradient in Burrard Inlet was still present, with dense water (22·4) at the bottom of station 60, so the possibility of inflow still existed. The mid-water temperature maximum which existed in February turned into a mid-water temperature minimum as a result of spring warming.

From March to May 1985, there were no further inflow events. The stratification in the upper 50 m of the water column gradually increased but there was little change in the deepwater properties. The temperature and density data show that the exchange which began in late December was over by March. Because they are monthly, however, these data do not provide information about the control and precise timing of the exchange. In the next section cyclesonde data are used to investigate the dynamics of the exchange in greater detail.

Forcing of the deepwater exchange

The timing of the exchange events is expected to be controlled by the tide, freshwater inflow, the wind and the density outside First Narrows. Energy is required to lift the dense water up over the sill of Indian Arm. In determining the source water for the exchange, it is important to determine from what depth the flow is capable of drawing water. This phenomenon is known as blocking and occurs in a number of different situations (Gill, 1982). The Bernoulli equation can be used to relate the blocking height h to the mean flow and the stratification.

$$\frac{p_1}{\rho} + \frac{u_1^2}{2} = \frac{p_2}{\rho} + gh + \frac{u_2^2}{2}. \tag{7}$$

The left side of equation (7) gives the kinematic energy of the approaching flow. The right side gives the energy of this water after reaching the top of the barrier. Water at the top of the barrier has increased potential kinematic energy gh, where g is the acceleration due to gravity. It is assumed that the flow at the top of the barrier has no remaining kinetic energy so $u_2 = 0$. If the average density of the surrounding water through which the water parcel moves is ρ_s then

$$p_1 - p_2 = \rho_s g h, \tag{8}$$

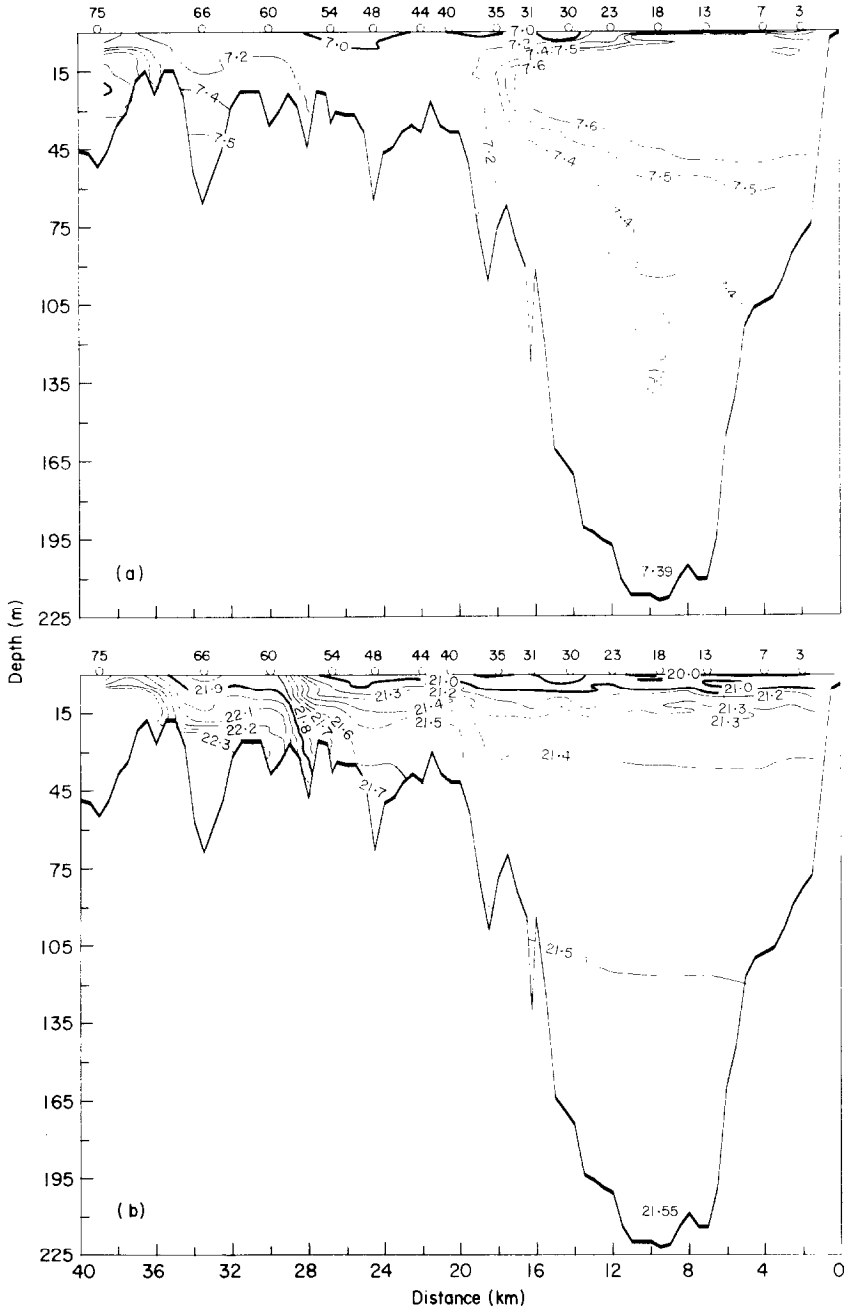

Figure 7. Temperature (a) and σ_t (b) along Indian Arm on 19 February 1985. The station numbers where the data were collected are indicated at the top of the plots.

and equation (7) becomes

$$gh\left(\frac{\rho-\rho_s}{\rho}\right)=\frac{u_1^2}{2}. \tag{9}$$

The density difference can be written in terms of the observed stratification which is assumed to be linear in z. Since ρ_s is the average density, for an approximately linear gradient ρ_s is reached for a height change of $h/2$.

$$\frac{\rho - \rho_s}{\rho} \simeq \frac{-1}{\rho}\left(\frac{\partial \rho}{\partial z}\right)\frac{h}{2} = \frac{N^2 h}{2g}, \tag{10}$$

where N is the buoyancy frequency. Inserting equation (10) into equation (9) gives the blocking depth

$$h = \frac{u_1}{N}. \tag{11}$$

The form of this equation can also be obtained from dimensional analysis as one expects the blocking depth to be a function of the stratification and the velocity. Any dissipation in the sill region will lead to a reduction in the blocking depth because of energy loss from the flow. Estuarine flow, leading to a non-zero u_2, will also lead to a reduction in the blocking depth. The blocking depth determined from equation (11) should be treated as an upper bound estimate.

The stratification and flow speed which control the blocking at the entrance to Burrard Inlet are approximately known. Outside First Narrows the estimated tidal velocity ranges from $0{\cdot}6\,\mathrm{ms}^{-1}$ to $1{\cdot}0\,\mathrm{ms}^{-1}$. For the winter of 1984/85, the buoyancy frequency N was about $0{\cdot}014\,\mathrm{s}^{-1}$. From equation (11), the blocking depth is 40–70 m; therefore the blocking depth is much deeper than the depth of the sills and thus water from the bottom of station 75, outside First Narrows, will not be blocked even during periods of neap tides. This result is important in showing that the source water for the exchange is available throughout the spring/neap tidal cycle.

Figure 8 shows the annual variation of water properties in the Strait of Georgia. Waldichuk (1957) discussed the deepwater renewal process in the Strait, a problem investigated in more detail by Samuels (1979). In the winter, water mixes in the passages leading into the Strait and sinks down into the deeper part of the Strait. In the summer, water enters the Strait reaching neutral buoyancy at mid-depths. Samuels interpreted this process to be very regular, subject to occasional intensification, rather than one where strong intermittent overturns occurred.

The source water for the Indian Arm exchange is probably in the top 100 m of the Strait of Georgia (Pickard, 1975). Figure 8 shows that the maximum salinity (or density) occurs late in the year. This timing is undoubtedly a controlling factor of the exchange in Indian Arm, as a comparison of water properties makes clear. The time series in Figure 3 shows that exchange in Indian Arm occurs just after the time of maximum density at 100 m in the Strait of Georgia.

In Figure 9 some of the data for the 1984/85 winter are presented. An estimate of the tidal kinetic energy per unit volume is plotted, together with the observed density and current data. The tidal kinetic energy is calculated from the tidal height data. Harmonic analysis of the sea level height yielded the various constituents which were used, together with data on the geometry of the sill, to determine the barotropic tidal velocity over the sill. A 24-h running average of the kinetic energy term was taken to allow visualization of the changing energy level available for mixing.

The 1984/85 record shows the effects of the tide during a period of bottom water renewal. Four strong renewal events are observed in the basin 170 m velocity record: at

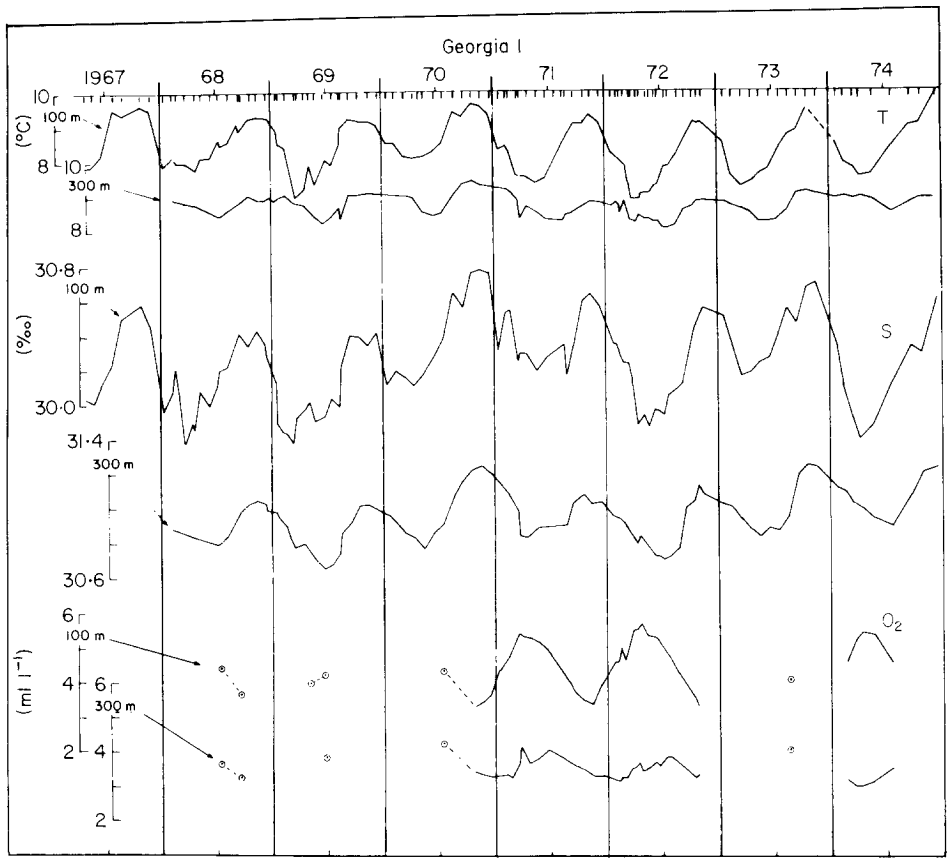

Figure 8. Long-term variation of temperature, salinity and DO_2 at 100 and 300 m depth in the Strait of Georgia. The station location G1 in the strait is 15 km west of station 75 (see Figure 1). From Pickard (1975).

days 380, 395, 405 and 435. Three of these events (at days 380, 395 and 435) have peak inflows which occur during neap tide. One (405) takes place just before the neap tide.

The inflow speed at the sill varied from 10–30 cm s^{-1}. Maximum inflow speeds at the sill on days 380, 395, 405 and 435 are associated, roughly at least, with the exchange events and with the neap tide. Large basin velocities, up to 10 cm s^{-1}, occur during these inflow events. Increases in the density at the bottom of the basin are also observed. The density at the sill shows distinct maxima not apparent in the basin record. The peaks in the density at the sill are associated with strong up-inlet flows in the basin. The density at the sill increases until the inflowing water is dense enough to reach the bottom. The peak velocity in the basin lags the density increase observed at the sill by as much as 5 days. Most of the observed peaks are associated with the neap tides. Between days 410 and 440, however, the peaks seem to occur halfway between spring and neap tides. At this time the tidal excursion is sufficient to carry the dense water up to the sill, while the mixing is weak enough that the density will not be as greatly reduced as it would during spring tides.

Figure 9(b) also shows the freshwater flow for 1984/85. These data provide an explanation for the lack of an inflow at day 422. A strong surge of freshwater begins at day 400 and continues until day 440. From day 380 to 420, there is an increase in the density at the

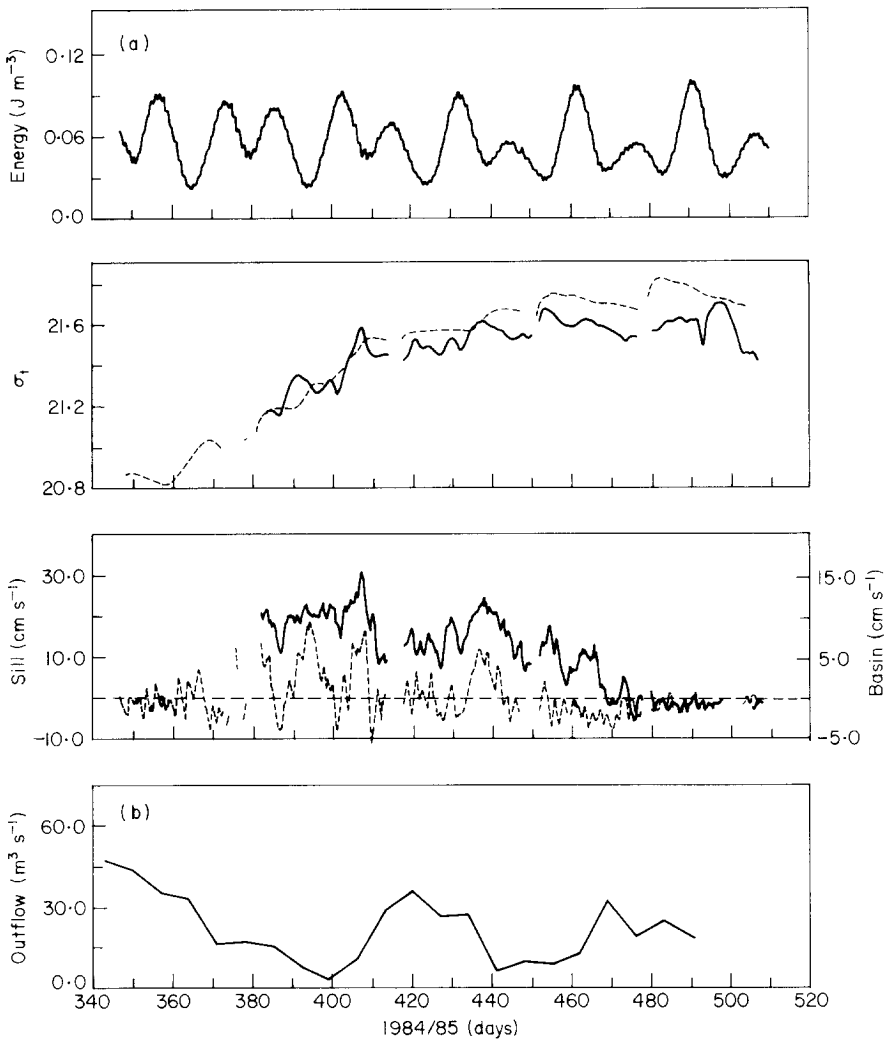

Figure 9. (a) Tidal energy, σ_t and along-channel current for the 1984/85 exchange. At the top is the tidal kinetic energy plotted as a 24-h average. The middle frame presents σ_t from the sill (C1: ———, 60 m) and basin (C3: - - - -, 170 m) stations. The bottom frame presents the along-channel current, with the tidal signal removed using harmonic analysis. Note that the basin and sill current data are plotted at different scales. Positive current is directed into the fjord, negative outwards. (b) Freshwater flow into Indian Arm, averaged over three-day intervals. Time is in Julian days from the start of 1984.

bottom of station 75, outside First Narrows. In spite of this density increase, there is no inflow of water at day 422. There is a drop in the density at the sill from day 410 to 435 associated with the freshwater surge.

The tidal excursion in Burrard Inlet is about 18 km, approximately the length of Burrard Inlet. If the tidal excursion in a shallow silled fjord is less than the sill length then mixing will be critically important since the water cannot make it over the sill on one tidal cycle. The water must be dense enough to reach the far end of the sill with sufficient negative buoyancy to sink. Bottom water renewal associated with neap tides has been observed in Puget Sound (Cannon & Laird, 1978; Geyer & Cannon, 1982) where the tidal

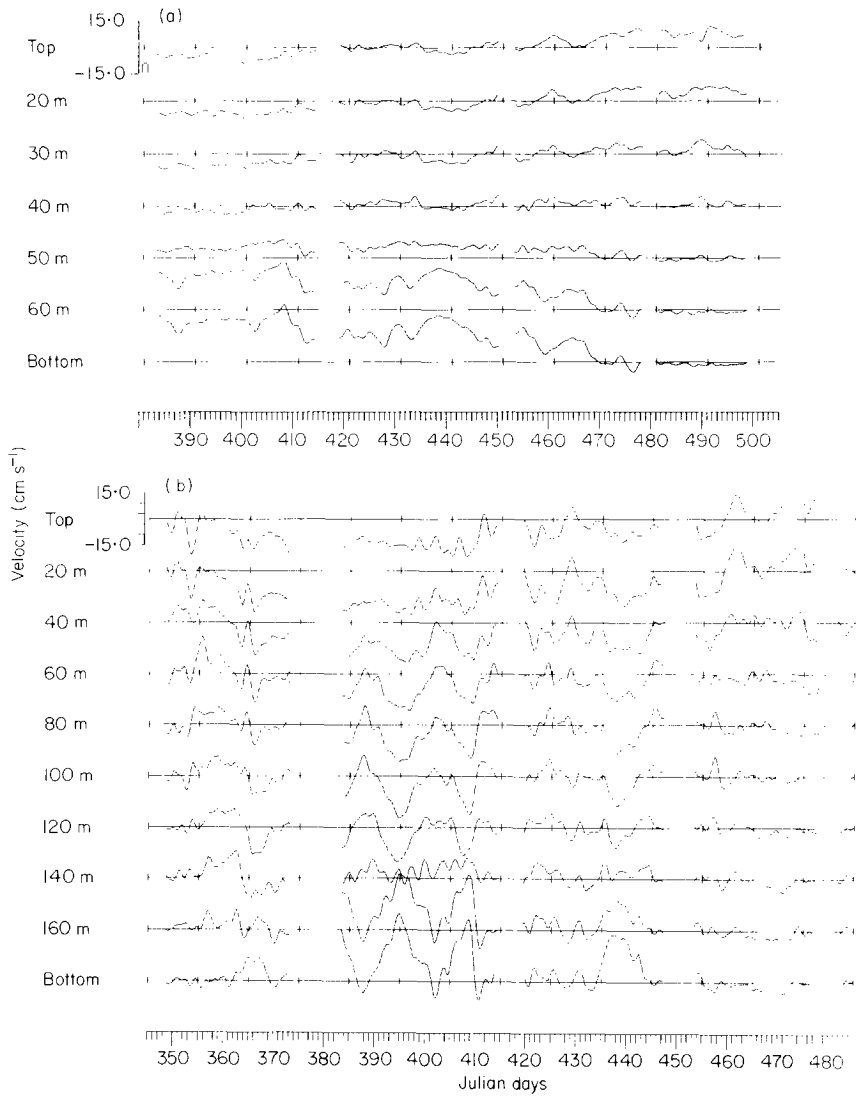

Figure 10. (a) Along-channel current at the sill (C1) in 1985. (b) Along-channel current at the basin (C3) in 1984/85. Positive currents (in cm s^{-1}) are directed into the fjord. The time scale is in Julian days from the start of 1984.

excursion is just slightly less than the length of the sill. In Rupert-Holberg Inlet, where the sill is short in comparison with the tidal excursion, exchange has been observed to be associated with spring tides (Drinkwater & Osborn, 1975; Stucchi & Farmer, 1976). In Indian Arm, with Burrard Inlet acting as the sill, mixing and the tidal excursion are crucial in determining the exchange timing.

Current averages during an exchange episode

The along-channel current in 1985 at C1 is shown in Figure 10(a). The cross-channel current is much weaker than the along-channel current (de Young, 1986) and is not

discussed. The data at the top and bottom in the plots are from the cyclesondes when positioned at either the top or bottom bumper. The top bumper was 14–20 m below the surface while the bottom bumper was 0–6 m deeper than the deepest depth plotted. The data at the 10 m depth intervals were found by linear interpolation, after first vector averaging the raw cyclesonde data over intervals of slightly less than 10 m, assuming that the heading varied linearly over the sampling interval. The current data in Figure 10 have had the M_2, S_2, N_2, K_1, O_1 and P_1 tides removed following harmonic analysis. The P_1 tide was determined using inference with the Vancouver Harbour tidal height record providing the amplitude ratio and phase difference information. A simple 24-h running average of the data was then done to reduce the noise level.

Complete renewal of the fjord occurred in 1984/85. Figure 10 shows the along-channel current at the sill and in the basin. The inflows at the sill hug the bottom; they appear to be about 20–30 m in thickness, an observation based upon the weakness of the inflow at 50 m and the depth of the station (70 m below datum). The strong inflows in the basin are 30–40 m thick during the two major inflow events between days 388 and 410. (The inflow is weak at 140 m and the station depth is 180 m below datum). Between the inflow events there is a reversal in the current at the bottom in the basin. Outflow is constant from the top to a depth of 40–50 m with pulses of outflow to 120 m depth at days 396–410.

Contoured along-channel currents in Figure 11(a) show the structure of the flow in the basin more clearly. The raw data were averaged over 25 h before contouring. The two large inflow events centered at days 30 and 44 [days 396–410 in Figure 10(b)] show mean bottom speeds as high as 10 cm s^{-1}. The zero crossing rises and falls with the inflow, dropping to a depth of 140 m during an exchange. The zero crossing at the sill [Figure 11(b)] during the same period does not change in depth appreciably. The sill inflow appears quite steady during the period, although there is some indication that the flow speeds up at day 44 but no evidence of this behaviour at day 30.

Data from the upper 20 m, Figures 11(b) and 12, came from four Aanderaa current meters suspended from a surface float, at depths of 3, 7, 11 and 15 m at station CS (see Figure 1). Data were also obtained from a cyclesonde current meter moored at station CS. A regression was made between the data from the cyclesonde at station CS and the cyclesonde from station C1. This regression was used to adjust the Aanderaa current meter data from station CS so that it would match the current data at station C1.

A contour plot of the raw data at the sill (Figure 12) indicates how the tidal flow changes there. Because the data are at 10 m depth intervals, some of the closed contours shown in Figure 12 must be interpreted with care. On strong floods there is inflow from the top to the bottom. On weak ebbs and floods, there is inflow below 50 m depth, stronger on the flood than on the ebb, with outflow above. On strong ebb tides there is outflow from the top to the bottom. Figure 12 shows that the flow is in phase during strong flood and ebb tides. These observations are in accord with those of Pickard and Rodgers (1959) in Knight Inlet where the observed flow at the sill was in phase from top to bottom.

Control of the exchange

Control of the deepwater exchange in Indian Arm depends on a variety of factors. The first condition requires water of sufficient density to be available outside the sill at First Narrows. This water must then make it over the sill and into Burrard Inlet. Mixing through Burrard Inlet will determine the density of this inflowing water at the Indian Arm sill. Control of the exchange can still be exerted between First Narrows and the Indian

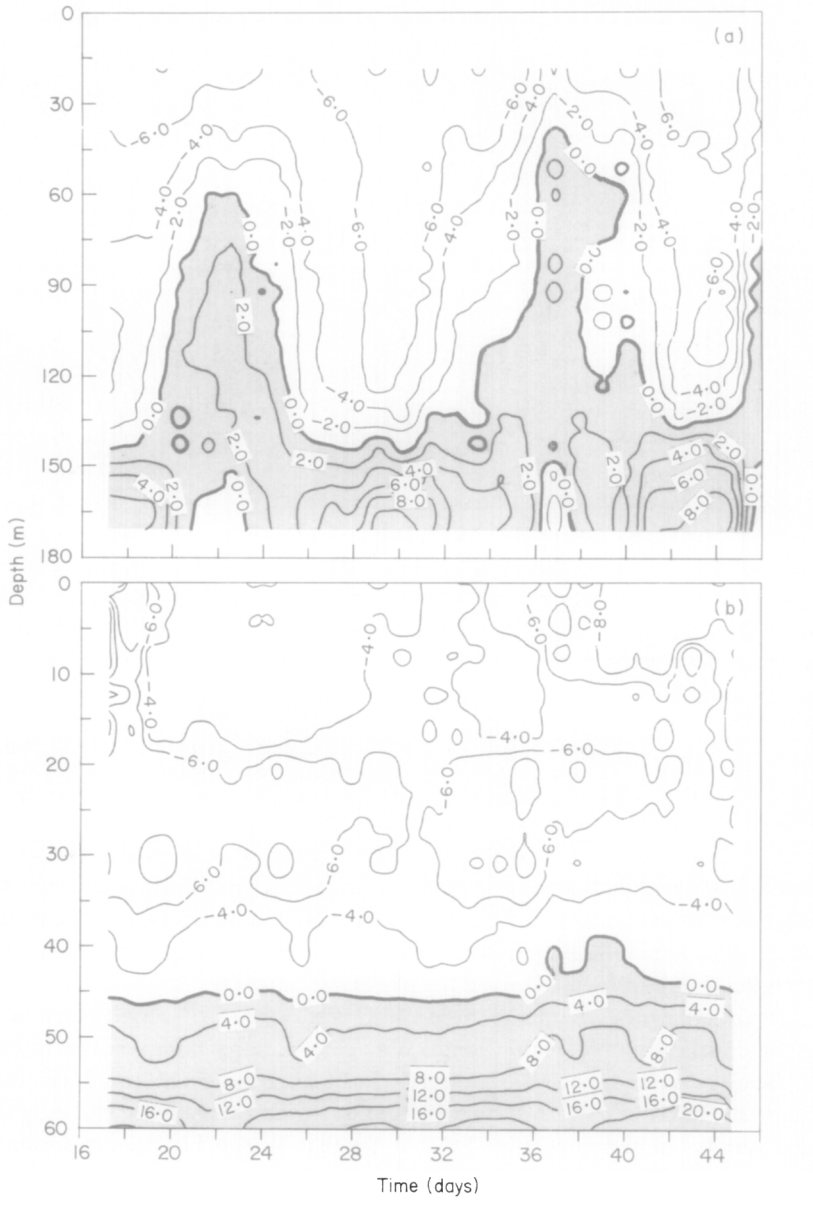

Figure 11. Contours of the along-channel current at the (a) basin (C3) and (b) sill (C1) stations. The data (in cm s^{-1}) are averaged over 25-h intervals. The time scale is in Julian days from the start of 1985. The inflows are shaded.

Arm sill where either hydraulic control or friction can control the exchange of water from outside the sill to inside the basin. A lack of data in the Burrard Inlet part of the system forces this discussion of control to be tentative.

Much work has been done on the nature of hydraulic control of flow in channels (see Turner, 1973). The first such work in estuaries was by Stommel and Farmer (1952, 1953) who looked at the effect of an abrupt change in the channel width on the flow. Farmer and

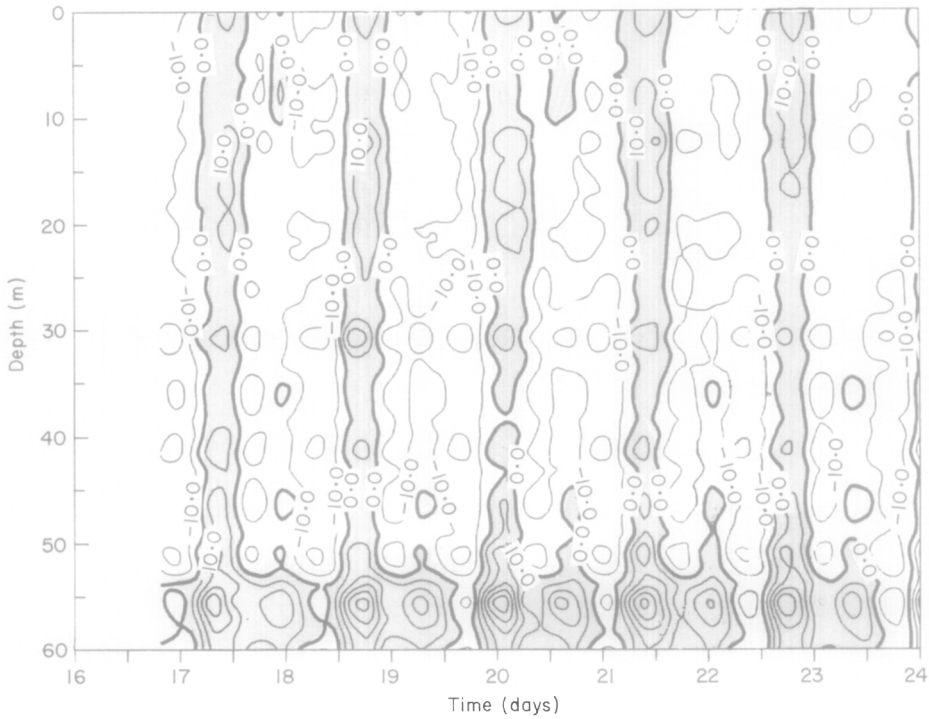

Figure 12. Contours of the along-channel current at the sill (C1) station in January 1985. The sampling interval for the data (in cm s^{-1}) is approximately 1·5 h. The time scale is in Julian days from the start of the year. Flow into the basin is shaded.

Armi (1986) show that the application of Stommel and Farmer's results to maximal two-layer exchange over a sill is incorrect. They show that either the sill or the contraction may act as the control, with different results in each case. Farmer and Armi (1986) also discuss the effects of barotropic flow on the exchange process.

In Indian Arm, which has three sills (First Narrows, Second Narrows and the Indian Arm sill, see Figures 1 and 2) and three contractions, complexities in the control of the exchange can be expected. Further complicating the geometry, is the third contraction, near the Indian Arm sill, which is about 1–2 km away from the sill. Some dynamical arguments can be made, however, that not all of Burrard Inlet is important in determining the control of the exchange.

Figure 13 shows a schematic of the exchange system as described by Farmer and Armi (1986), whose theoretical development is followed here. The flow will be considered to be two-layered, an assumption which is not always valid in Indian Arm, but may not be a bad one for the exchange problem where there is inflow of dense water and outflow of less dense basin water. The source of the dense water (Burrard Inlet) is on the right, with the basin (Indian Arm) on the left. The flow is said to be critical (Turner, 1973) when

$$G^2 = F_1^2 + F_2^2 = 1, \tag{12}$$

where $F_i^2 = U_i^2/g'y_i$ is the densimetric Froude number for layer i, U_i is the flow speed, y_i is the layer thickness and $g' = g\Delta\rho/\rho_2$ is the reduced gravity ($\Delta\rho = \rho_2 - \rho_1$). The upper and lower layers are indicated by the subscripts 1 and 2.

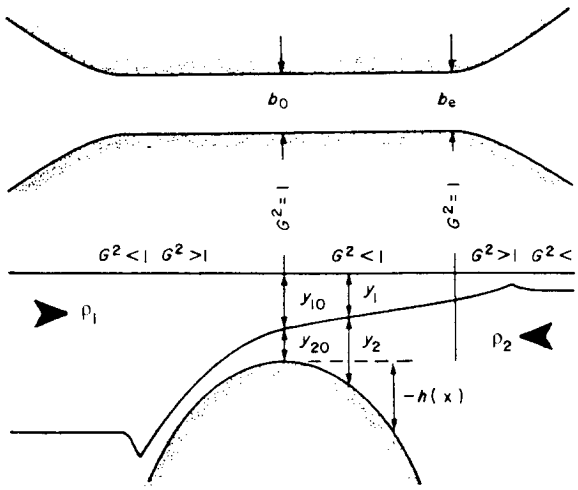

Figure 13. Schematic for maximal two-layer exchange over a sill. From Farmer and Armi (1986) by permission of Cambridge University Press.

In their discussion of the flow over a sill, Farmer and Armi (1986) use the Bernoulli equations and the Froude number for each layer. The combined Bernoulli equations are written in terms of the Froude numbers. They show that the interface height at the sill for maximal exchange, when the flow is supercritical on either side of the sill, is about 0·375 times the sill depth. If the flow is supercritical on only one side, the reservoir on that side can exert no control on the exchange.

Figure 6 shows the density in the basin on a tide which was just beginning to flood. The 21·0 isopycnal, which runs from outside Second Narrows to inside the basin, looks much like the interface trace presented in the schematic of Figure 13. The dip in the isopycnal on the far side of the sill can be explained as a hydraulic jump as the flow reverts to subcritical from supercritical. A calculation of the lower layer Froude number at the sill cyclesonde station shows it to be, $F_2^2 \geqslant 1$ (if $\Delta\rho \sim 0{\cdot}2$ and $U \sim 0{\cdot}4\,\mathrm{m\,s^{-1}}$); thus the conditions for supercritical flow on one side of the sill are met. At Second Narrows where the flow is greater than $1\,\mathrm{m\,s^{-1}}$, it is expected that the flow should be supercritical in spite of the stronger stratification there. Supercritical flow at these two points simplifies the analysis since it means that only the area between Second Narrows and the sill will be important in controlling the exchange.

The effect of the barotropic tide on the exchange process is also considered by Farmer and Armi (1986) who define a dimensionless barotropic speed U_0, which is scaled by $\sqrt{g'(y_1+y_2)_0}$. In Indian Arm, $|U_0|$ is about 1 in the neighbourhood of the sill and thus the schematics of Figure 14(b–h), taken from Farmer and Armi's barotropic analysis, should apply here in Indian Arm. These diagrams are based upon the solutions to the combined Bernoulli equations in the upper and lower layer with an imposed barotropic flow. As the tide moves from weak to strong flood [from (d) to (h) in Figure 14], the dense water moves over the sill forcing the upper layer Froude number in the basin of Indian Arm to zero. At maximum flood over the sill, there is only a single layer flowing over the sill. On ebb tide [from (d) to (b) in Figure 14], the water from the basin forces its way over the sill eventually establishing single layer flow over the sill in the opposite direction. Figure 12 supports this interpretation. On flood tide all of the flow is directed into the basin. On ebb tide the

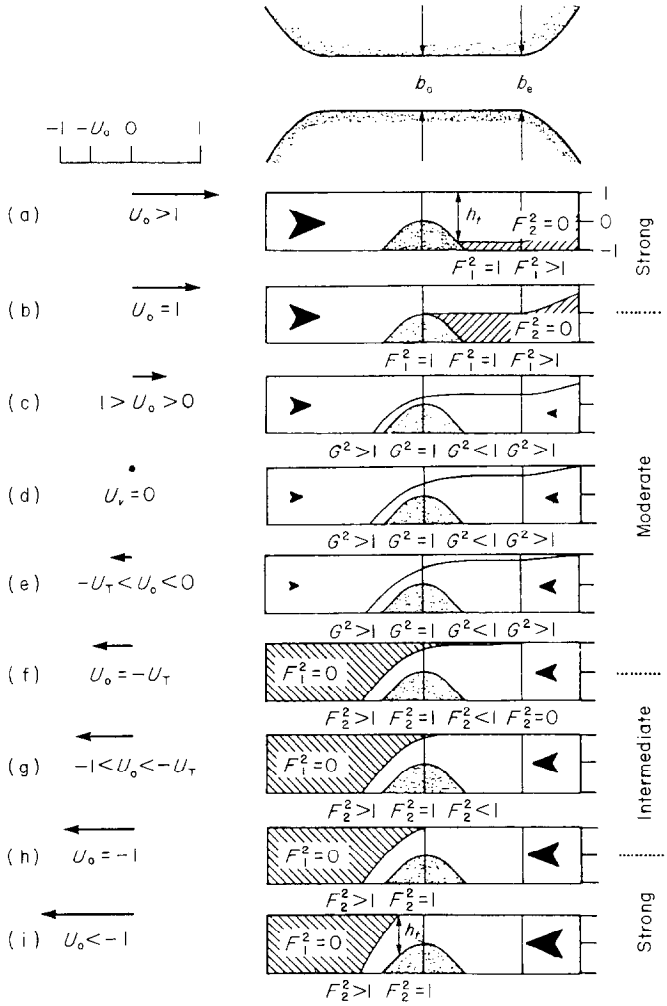

Figure 14. Scheme to show the exchange over a sill with a barotropic flow. The dimensionless barotropic speed, U_0, is indicated on the left. In Indian Arm, U_0 is about 1. From Farmer and Armi (1986), by permission of Cambridge University Press.

flow is arrested, though on weak ebbs the flow is not always arrested all the way to the bottom. The mean interface height at station C1 is 25 m which is 0·36 times the depth, providing remarkable agreement with the prediction of 0·375 based on maximal exchange (Farmer & Armi, 1986). In comparing these observations to theory, it must be remembered that the data in Figure 12 are from just inside the sill, about 40 m below sill depth at the bottom.

This brief comparison suggests that the theory of Farmer and Armi (1986) may be applicable to the Indian Arm exchange problem. The contractions in Indian Arm have been ignored in this discussion, but in reality may play an important role in controlling the exchange. Better information about the flow, and the Froude numbers, in the sill region is required to determine how important all these various factors might be. For two-layer flow, both bottom and interfacial friction must also be considered in determining the nature of the control. The influence of friction in long straits has been treated by Assaf and

TABLE 1. Period of duration, speed and thickness, transport and percentage volume of Indian Arm during bottom water renewal events of 1984/85

Period	Speed at C1 ($cm\ s^{-1}$)	Thickness (m)	Transport ($m^3\ s^{-1}$)	Indian Arm volume (%)
380–386	14	(25)	700	16
390–400	14	(25)	700	27
405–410	16	(25)	800	15
435–443	14	(25)	700	22

Hecht (1974); however, there is not enough information available here to apply their theory. If the flow at Second Narrows is supercritical, the rest of Burrard Inlet may be ignored. Only the 8 km from Second Narrows to the basin of Indian Arm would then be important. Over such a comparatively short distance, friction may not be important in controlling the exchange. Numerical modeling, with the application of reasonable friction coefficients at the bottom and at the interface between the two layers, might help to resolve the problem.

Transport estimates

There are many difficulties in estimating the transport in a fjord. Measurements from a depth of 3 m to within 10 m of the bottom were made at the sill of Indian Arm, but there is still a lack of near-surface measurements in the basin. The measurements at the sill do not extend all the way to the bottom and there is the further problem of cross-inlet variability. No measurements were made across the channel so it is impossible to estimate the effect of this factor. It is recognized, however, that sidewall friction and topographic effects may be important in determining the extent of any variation across the channel.

In this section, an estimate of the transport and volume of the 1984/85 exchange events is made. The sill record [Figure 10(a)] does not differentiate the inflow periods clearly enough to allow determination of the duration of the inflow. However, the sill data will be useful, in computing the transport because it is at the sill that the inflowing water enters Indian Arm. The period of the exchange events can be determined from the basin data [Figure 10(b)] which clearly show when the exchanges occurred. It is not possible to judge the transport of the exchange from the basin data, however, because of entrainment into the flow which occurs when the dense water moves down the slope from the sill into the basin.

Table 1 shows the estimated characteristics of the four main inflow events which occur during the winter of 1984/85. The values given in this table were estimated from analysis of Figures 10(a) and 10(b) showing the current at the sill and the basin. The period of renewal varies from 5–10 days in length. Flow speeds at the sill are fairly constant during the renewal, although this is not true in the basin where a distinct peak can be seen. As the tidal energy decreases during the renewal, the density increases and the speed of the density current flow into the basin reaches a maximum.

The vertical resolution of the current data at the sill is such that the estimated flow thickness is not well known. The current data in Figure 10 do indicate, however, that this thickness does not change much in the early winter of 1985. The average thickness is about

25 m. The speed in Table 1 is an average taken over the inflow. The width of the channel, which is U-shaped, was determined from bathymetric charts. The mean width over the inflow was 200 m. Above the inflow the mean width was 500 m. Taking into account the ratio of the cross-sectional areas, it can be seen that to maintain continuity the return flow need only have been [25(200)]/[45(500)] = 0·22 times the inflow speed. Figure 11(b) shows that the measured speed, about 5 cm s^{-1}, is close to the expected speed of 3 cm s^{-1}. The percentage volume estimates show that nearly all the water in Indian Arm was exchanged during the 1984/85 winter. About one-fifth of the inlet was overturned during each exchange event.

The inflow of the water down the slope will take place as a density current (Ellison & Turner, 1959; Benjamin, 1968; Bo Pedersen, 1980). The density difference provides the negative buoyancy force that drives the flow down the slope. Three other factors control the flow speed: (1) the thickness of the flow, (2) the angle of the slope and (3) the friction the current feels (both at the bottom and the top of the layer) as it moves down the slope. The equation describing this relationship has been derived by a number of workers (for example Bo Pedersen, 1980):

$$U = \left(\frac{g\left(\frac{\rho' - \rho}{\rho'}\right) h \sin\beta}{\frac{f}{2}} \right)^{\frac{1}{2}} \tag{13}$$

where h is the flow thickness, g the acceleration due to gravity, β the angle of the slope, ρ' the density of the inflow, ρ the density of the overlying water and $f/2$ a dimensionless friction parameter. From the January 1985 CTD survey $\Delta\rho \approx 0{\cdot}1$ kg m^{-3}, the bottom slope is 0·0185 and h is about 25 m. In his review of the literature, Bo Pedersen (1980) estimated the dimensionless friction parameter $f/2$ to span the range $2 \times 10^{-3} < f/2 < 3 \times 10^{-2}$. Substituting into equation (13) one finds that U should span the range $12 < U(\text{cm s}^{-1}) < 46$ (depending upon the friction coefficient), in fair agreement with the observations.

Close inspection of the basin and sill velocities indicates that the basin velocity lags the sill velocity by as much as one day. This result is consistent with a velocity of the density current down the slope of 10 cm s^{-1}. As the density current penetrates deeper into the fjord, the density difference may be expected to decrease and thus a slower speed might be expected.

Summary

The deepwater exchange cycle in Indian Arm has been described. It has been shown that, once high density water is available at the entrance to the system, the timing of the exchange is controlled by the spring/neap tidal cycle. The timing of the exchange, associated with spring-neap tidal effects, has been observed in other fjord systems (Drinkwater & Osborn, 1975; Geyer & Cannon, 1982). During neap tides, when reduced energy for mixing is available, the water reaching the sill attains a maximum in density. Spring tides reduce the density of the water reaching the sill because of the increased energy available for mixing. Freshwater flow was observed to prevent the exchange during one spring/neap tidal period. Each exchange episode, associated with the neap tidal period, lasted for 5–10 days. Approximately 20% of the basin water was exchanged during each episode. The 1984/85 winter exchange took place in four distinct episodes starting in late December and ending in mid-March.

The observations of the flow are consistent with hydraulic control theory (Farmer & Armi, 1986). The inflow exhibits maximal exchange conditions with supercritical flow on

either side of the sill. Current meter observations, from just inside the sill, are consistent with the hydraulic control explanation. Better data are required to test the theory more completely. Current and density data from Burrard Inlet were lacking. The nature of the flow through this section is crucial in determining how the exchange is controlled. Improved observations might also allow some determination of the effect of the complex channel topography upon the inflow. The agreement presented here between the observations and the theory suggests that the channel irregularities are not important.

An important feature of the exchange process is the diffusion of salt and temperature which condition the basin water, by lowering the density, to set up conditions for the next overturning. In a budget analysis of the salinity and temperature data, it was found that the vertical diffusion constant K_v was related to the buoyancy frequency N ($K_v \propto N^{-1.6}$). In another British Columbia inlet, a different slope was found, $K_v \propto N^{-1.8}$. The theory of Gargett and Holloway (1984) suggests $K_v \propto N^{-1}$ if the energy source for the diffusion is an internal wave field of single frequency. The differences between the observations and the theory may be accounted for if there are other energy sources for the diffusion.

Acknowledgements

For the suggestion of the Bernoulli equation analysis of the blocking, we are grateful to Dr I. Gartshore. Technical assistance came from many people including A. Ramnarine, M. Storm, D. English, R. Bigham, A. Stickland, J. Love, K. Thomson and H. Heckl. The officers and crews of the *C.S.S. Vector* and the *C.N.A.V. Endeavour* provided the platforms from which all of the data were collected. Computer software for much of the data translation came from D. Laplante, V. Lee and D. Dunbar. V. Lee also helped perform some of the drudgery involved in cleaning up the cyclesonde files. We also thank the reviewer who found an error in the original diffusion analysis. The Natural Sciences and Engineering Research Council provided support for this project, in the form of an operating grant (A-8301) to S.P. and a scholarship to B.deY.

References

Anderson, J. J. & Devol, A. H. 1973 Deep water renewal in Saanich Inlet, an intermittently anoxic basin. *Estuarine and Coastal Marine Science* **1**, 1–10.

Assaf, G. & Hecht, A. 1974 Sea straits: a dynamical model. *Deep-Sea Research* **21**, 947–958.

Benjamin, T. B. 1968 Gravity currents and related phenomena. *Journal of Fluid Mechanics* **31**, 20–48.

Bo Pedersen, F. 1980 *A Monograph on Turbulent Entrainment and Friction in Two-layer Stratified Flow.* Institute of Hydrodynamics and Hydraulic Engineering, Technical University of Denmark.

Burling, R. W. 1982 Deep circulations in inlets: Indian Arm as a case study. In *Marine Tailings Disposal* (Ellis, D. V. ed.). Ann Arbor Science, Ann Arbor, Michigan, pp. 85–132.

Cannon, G. A. & Laird, N. P. 1978 Variability of currents and water properties from year long observations in a fjord estuary. In *Hydrodynamics of Estuaries and Fjords* (Nihoul, J. ed.). Elsevier, Amsterdam.

Davidson, L. W. 1979 On the physical oceanography of Burrard Inlet and Indian Arm. M.Sc. Thesis, University of British Columbia, Vancouver, British Columbia.

de Young, B. 1986 The circulation and internal tide of Indian Arm, B.C. Ph.D. Thesis, University of British Columbia, Vancouver, British Columbia.

de Young, B. & Pond, S. 1987 The internal tide and resonance in Indian Arm. *Journal of Geophysical Research* **92**, 5191–5207.

Drinkwater, K. F. & Osborn, T. R. 1975 The role of tidal mixing in Rupert and Holberg Inlets, Vancouver Island. *Limnology and Oceanography* **20**, 518–529.

Dunbar, D. S. 1985 A numerical model of stratified circulation in a shallow-silled inlet. Ph.D. Thesis, University of British Columbia, Vancouver, British Columbia.

Ellison, T. H. & Turner, J. S. 1959 Turbulent entrainment in stratified flows. *Journal of Fluid Mechanics* **6**, 423–448.

Farmer, D. M. & Armi, L. 1986 Maximal two-layer exchange over a sill and through the combination of a sill and contraction with barotropic flow. *Journal of Fluid Mechanics* **164,** 53–76.

Farmer, D. M. & Freeland, H. J. 1983 The physical oceanography of fjords. *Progress in Oceanography* **12,** 147–220.

Gade, H. G. & Edwards, A. 1980 Deep water renewal in fjords. In *Fjord Oceanography* (Freeland, H. J., Farmer, D. M. & Levings, C. D. eds). Plenum Press, New York, pp. 453–489.

Gargett, A. E. 1984 Vertical diffusivity in the ocean interior. *Journal of Marine Research* **42,** 359–393.

Gargett, A. E. & Holloway, G. 1984 Dissipation and diffusion by internal wave breaking. *Journal of Marine Research* **42,** 15–27.

Geyer, W. R. & Cannon, G. A. 1982 Sill processes related to deepwater exchange in a fjord. *Journal of Geophysical Research* **87,** 7985–7996.

Gill, A. E. 1982 *Atmosphere-Ocean Dynamics*. Academic Press, New York.

Gilmartin, M. 1962 Annual cyclic changes in the physical oceanography of a British Columbia fjord. *Journal of the Fisheries Research Board of Canada* **19,** 921–974.

Lewis, E. L. & Perkin, R. G. 1982 Seasonal mixing processes in an Arctic fjord system. *Journal of Physical Oceanography* **12,** 74–83.

Munk, W. H. 1981 Internal waves and small scale processes. In *Evolution of Physical Oceanography* (Warren, B. A. & Wunsch, C. eds). MIT Press, Cambridge, MA, pp. 264–271.

Osborn, T. R. 1980 Estimates of the local rate of vertical diffusion from dissipation measurements. *Journal of Physical Oceanography* **10,** 83–89.

Pickard, G. L. 1961 Oceanographic features of inlets in the British Columbia mainland coast. *Journal of the Fisheries Research Board of Canada* **18(6),** 907–999.

Pickard, G. L. 1975 Annual and longer term variations of deepwater properties of the coastal waters of southern B.C. *Journal of the Fisheries Research Board of Canada* **32,** 1561–1587.

Pickard, G. L. & Rodgers, K. 1959 Current measurements in Knight Inlet, B.C. *Journal of the Fisheries Research Board of Canada* **16(5),** 635–678.

Samuels, G. 1979 A mixing budget for the Strait of Georgia, British Columbia. M.Sc. Thesis, University of British Columbia, Vancouver, British Columbia.

Stigebrandt, A. 1976 Vertical diffusion driven by internal waves in a sill fjord. *Journal of Physical Oceanography* **6,** 486–495.

Stigebrandt, A. 1980 Some aspects of tidal interaction with fjord constrictions. *Estuarine and Coastal Marine Science* **11,** 151–166.

Stommel, H. & Farmer, H. G. 1952 Abrupt changes in width in two-layer open channel flow. *Journal of Marine Research* **11,** 205–214.

Stommel, H. & Farmer, H. G. 1953 Control of salinity in an estuary by a transition. *Journal of Marine Research* **12,** 13–20.

Stucchi, D. & Farmer, D. M. 1976 Deepwater exchange in Rupert-Holberg Inlet. *Pacific Marine Sciences Report, 76-10,* Institute of Ocean Sciences, Patricia Bay, British Columbia.

Turner, J. S. 1973 *Buoyancy Effects in Fluids*. Cambridge University Press, Cambridge.

van Leer, J. C., Düing, W., Enrath, R., Kennelly, E. & Speidel, A. 1974 The Cyclesonde: an unattended vertical profiler for scalar and vector quantities in the upper ocean. *Deep-Sea Research* **21,** 385–400.

Waldichuk, M. 1957 Water exchange in Port Moody, British Columbia and its effect upon waste disposal. *Journal of the Fisheries Research Board of Canada* **22(3),** 801–822.